'90 KACC 1990. 10. 26~27

High Performance Torque Control of Induction Motor by Speed Sensorless Vector Control

Fumio Harashima *, Seiji Kondo *
and Shuji Inoue **
*Institute of Industrial Science, University of Tokyo
7-22-1, Roppongi, Minato-ku, Tokyo 106, JAPAN
**Drive System Div., Sumitomo Heavy Industries Co., Ltd
731-1, Naganumahara-cho, Chiba 281, JAPAN

Abstract

A method of speed sensorless vector control of induction motor is proposed in this paper. This method uses the slip frequency estimated by only the primary voltage and current. As this slip frequency accords with the command value of it, the commanded primary frequency is controlled. The validity of the method is confirmed by the simulation and experimental results.

1. Introduction

The vector control of an induction motor with slip frequency control is employed in industrial applications. The conventional vector control requires a speed sensor, which causes the following problems:

(1) As the shaft encoder is a delicate mechanical device, the careful treatment is necessary. (ex. very high speed application such as spindle drives)
(2) One side of motor shaft can not be used, because it is used for the attachment of the speed sensor. (ex. rotary press)
(3) The conventional vector control is not applicable to special applications where a speed sensor can not be used. (ex. elevator for construction work)

One of solutions for these problems is development of speed sensorless vector control. ([1],[2],[3],[4])

This paper proposes a speed sensorless vector control system. In the system, the slip frequency is estimated by only the primary voltage and current. The effectiveness of the proposed control method is verified by simulation and experimental results.

2. Outline of Slip Frequency Type Vector Control with Rotor Speed Sensor ([5],[6],[7])

Assuming that the rotor angular speed ω_r can be detected by a speed sensor, it is well known that very fast torque response of on induction motor can be achieved by controlling the primary angular frequency ω_1^* and the magnitude of primary current $|i_1^*|$, as follows:

$$\omega_1^* = \omega_r + \omega_s^* \tag{1}$$

$$|i_1^*| = \sqrt{(I_{1d}^*)^2 + (I_{1q}^*)^2} \tag{2}$$

$$\omega_s^* = R_2 \frac{T_q^*}{(\Phi^*)^2} \tag{3}$$

$$I_{1d}^* = \frac{\Phi^*}{M} \tag{4}$$

$$I_{1q}^* = \frac{L_2}{M} \frac{T_q^*}{\Phi^*} \tag{5}$$

where Φ^* and T_q^* are the commanded values of the secondary flux and the motor torque. If the vector control is successfully realized, the arrangement of primary current vector i_1^* becomes as shown in Fig1. It should be noticed here that the direction of the d*-axis coincides with that of the actual secondary flux and those rotate at angular speed ω_1^*. From Fig.1 and Eqs. (3)-(5), the phase difference θ^* between i_1^* and d*-axis holds the following relation:

$$\theta^* = \tan^{-1} \frac{I_{1q}^*}{I_{1d}^*} = \tan^{-1} \frac{L_2}{R_2} \omega_s^* \tag{6}$$

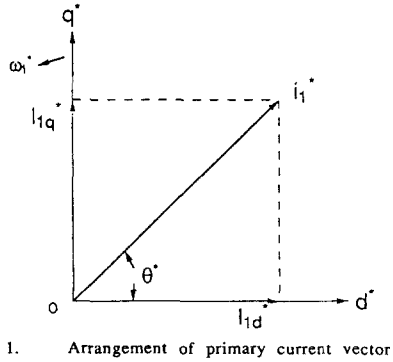

Fig. 1. Arrangement of primary current vector on rotating d-q coordinates

3. Method of Speed Sensorless Vector Control

The most important point to achieve fast torque response is to make the direction of the d*-axis coincide with that of the actual secondary flux. This means that $\theta = \theta^*$ should be achieved. From Eq. (6), the condition holds if $\omega_s = \omega_s^*$ is realized.

For the explanation of the proposed method of speed sensorless vector control, it is assumed that the estimated value of slip frequency $\widehat{\omega_s}$ can be obtained without any speed sensor. This method will be shown later on. If $\omega_s = \widehat{\omega_s}$ and it is possible to make $\widehat{\omega_s} = \omega_s^*$, the vector control can be realized.

3.1 Method of making $\widehat{\omega_s} = \omega_s^*$

As one of the control rules to make $\widehat{\omega_s} = \omega_s^*$, we propose the following PI-control rule:

$$\omega_1^* = K_P(\omega_s^* - \widehat{\omega_s}) + K_i \int (\omega_s^* - \widehat{\omega_s})\,dt \qquad (7)$$

K_P: proportional gain
K_i: integral gain

Assuming $\omega_s = \widehat{\omega_s}$, the validity of this method will be examined as follows.

(i) in the case: $\widehat{\omega_s} < \omega_s^*$

The arrangement of reference value and actual value is shown in Fig. 2 where the rotating d-q coordinates are used. As shown in Fig. 2, $i_1 = i_1^*$ holds because the minor control of primary current is used. Refering the relation of Eq. (6), it is understood that if $\widehat{\omega_s} < \omega_s^*$ then $\theta < \theta^*$. In this case, the phase of d*-axis is delayed from d-axis which is the direction of the actual flux. Therefore, the increase of ω_1^* by Eq. (7) accelerates the rotation speed of d*-axis and is effective to make $\theta = \theta^*$.

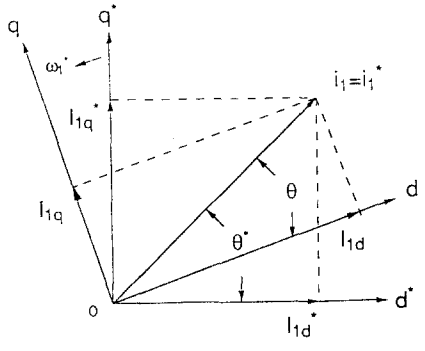

Fig. 2. Arrangement of actual and reference coordinates ($\widehat{\omega_s} < \omega_s^*$)

(ii) in the case: $\widehat{\omega_s} > \omega_s^*$

The arrangement of actual value and reference value in this case is shown in Fig. 3. The phase of d*-axis goes ahead of d-axis. Then the decrease of ω_1^* by Eq. (7) is effective to make $\theta = \theta^*$.

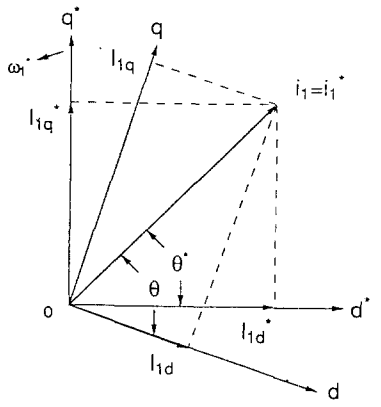

Fig. 3. Arrangement of actual and reference coordinates ($\widehat{\omega_s} > \omega_s^*$)

(iii) in the case: $\widehat{\omega_s} = \omega_s^*$

As shown in Fig. 4, each phase of d*-axis and d-axis is the same. Then the value of ω_1^* is kept constant by Eq. (7).

From these discussions, the effectiveness of the control rule Eq. (7) is qualitatively verified.

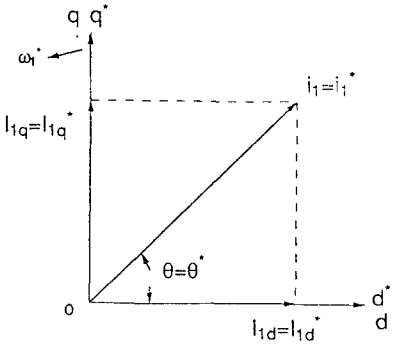

Fig. 4. Arrangement of actual and reference coordinates ($\widehat{\omega_s} = \omega_s^*$)

3.2 Estimation method of $\widehat{\omega_s}$

The estimation method of $\widehat{\omega_s}$ is derived from the voltage and current equation of an induction motor on the stationary coordinates (α-β axis):

$$\begin{pmatrix} v_1 \\ 0 \end{pmatrix} = \begin{pmatrix} (R_1 + L_\sigma p)\,I & \frac{M}{L_2} p\,I \\ -\frac{M R_2}{L_2} I & \left(\frac{R_2}{L_2} + p\right) I - \omega_r J \end{pmatrix} \begin{pmatrix} i_1 \\ \varnothing_2 \end{pmatrix} \qquad (8)$$

$$p = \frac{d}{dt}, \qquad L_\sigma = \frac{L_1 L_2 - M^2}{L_2}$$

$$I = \begin{pmatrix} 1 & 0 \\ 0 & 1 \end{pmatrix}, \qquad J = \begin{pmatrix} 0 & -1 \\ 1 & 0 \end{pmatrix}$$

The generated torque T_q is given as:

$$T_q = -\frac{M}{L_2} \varnothing_2^T J \, i_1 \tag{9}$$

Integrating both sides of the first row of Eq. (8) and solving with respect to $\varnothing_2$, yields the equation to calculate $\varnothing_2$:

$$\varnothing_2 = \frac{L_2}{M} \left\{ \int (v_1 - R_1 i_1) dt - L_\sigma i_1 \right\} \tag{10}$$

In what follows, the relation between ω_s and T_q will be derived from the second row of Eq. (8). Multiplier the second row of Eq. (8) by $(J \varnothing_2)^T$, using the identical equation $\varnothing_2^T J^T \varnothing_2 = 0$, and introducing Eq. (9), we may obtain

$$0 = -R_2 T_q + \varnothing_2^T J^T (p \varnothing_2) - \omega_r |\varnothing_2|^2 \tag{11}$$

The second term of the right hand side of Eq. (11) can be rewritten as:

$$\varnothing_2^T J^T (p \varnothing_2) = \varnothing_2^T J^T \left\{ \frac{d|\varnothing_2|}{dt} \cdot \frac{\varnothing_2}{|\varnothing_2|} + \omega_{\varnothing_2} J \varnothing_2 \right\}$$

$$\equiv \omega_1 |\varnothing_2|^2$$

where $\omega_{\varnothing_2}$ is the angular speed of $\varnothing_2$, and the relation $\omega_{\varnothing_2} = \omega_1$ which is valid in the successful vector control system has been used. Substitution of the above approximation into Eq. (11) leads to the desired relation between ω_s and T_q:

$$\omega_1 - \omega_r = \omega_s = R_2 \frac{T_q}{|\varnothing_2|^2} \tag{12}$$

In Eqs. (9), (10) and (12), the calculated values are identified by the symbol ^ :

$$\widehat{\varnothing_2} = \frac{L_2}{M} \left\{ \int (v_1 - R_1 i_1) dt - L_\sigma i_1 \right\} \tag{13}$$

$$\widehat{T_q} = -\frac{M}{L_2} \widehat{\varnothing_2}^T J \, i_1 \tag{14}$$

$$\widehat{\omega_s} = R_2 \frac{\widehat{T_q}}{|\widehat{\varnothing_2}|^2} \tag{15}$$

These equations give the estimation method of $\widehat{\omega_s}$, and use only v_1 and i_1, but does not use ω_r.

3.3 Simulation result

The effectiveness of the proposed method was examined by the simulation. Fig. 5 shows the block diagram of speed sensorless vector control system. In this diagram, the reference values ω_s^*, I_{1d}^*, I_{1q}^* are determined by Eqs. (3)-(5), ω_1^* is determined by Eq. (7), and $\widehat{\omega_s}$, $\widehat{T_q}$, $\widehat{\varnothing_2}$ are calculated by Eq. (13)-(15). The motor constants are listed in Table 1.

The simulation result of dynamic response to the stepwise change of torque command T_q^* is shown in Fig. 6. The actual slip frequency ω_s is in very good accordance with the reference slip frequency ω_s^*. It is examined by the simulation result that the proposed method of speed sensorless vector control works very well.

Only the method presented above, however, is not enough to realize an experimental system. Small modification of Eq. (13) should be made and will be presented in the next chapter.

Table 1 Motor Constants

3 phase , 4 pole
Power 0.9 kW
M :112.2 mH
L1 :114.5 mH , L2 :115.9 mH
R1 :1.03Ω , R2 :0.909 Ω (at 115 °C)

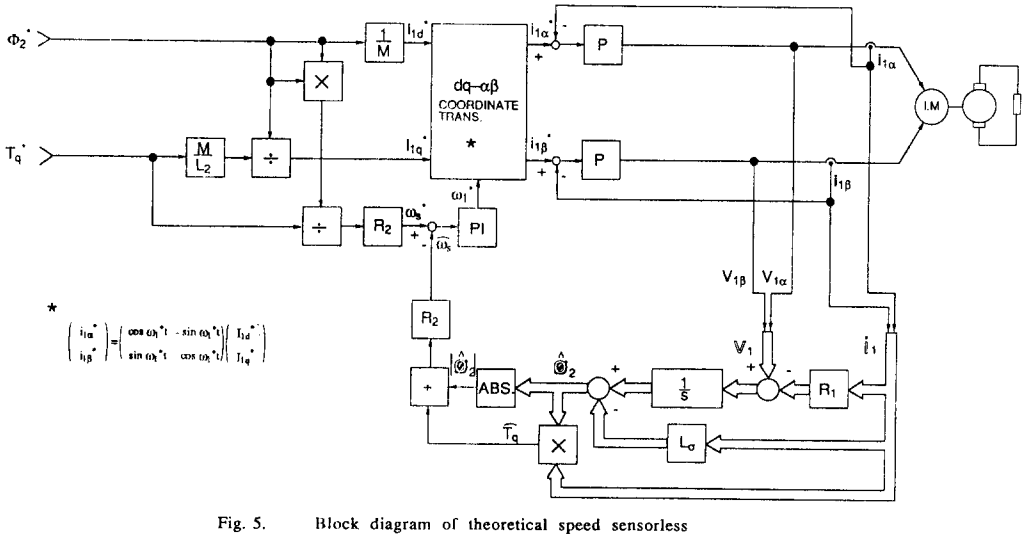

Fig. 5. Block diagram of theoretical speed sensorless torque control system

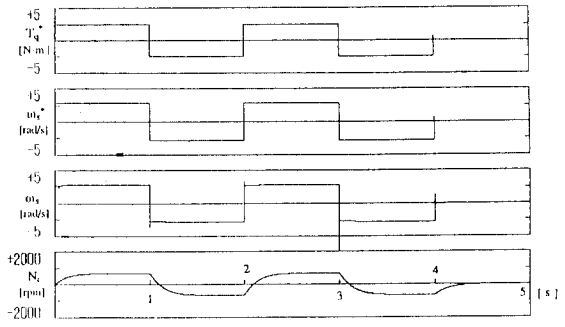

Fig. 6. Simulation result of torque control

4. Experimental Results

4.1 Experimental system

One problem for the practical application of the proposed method arises from the integration in Eq. (13). Since there inevitably exist very small offset errors in the detected signals of v_1 and i_1, the pure integration in Eq. (13) causes saturation problem. Therefore, the pure integration is replaced by a first order lag filter. Then, Eq. (13) is modified into the following expression:

$$\widehat{\Phi_2} = \frac{M}{L_2}\left\{\frac{T}{sT+1}(v_1 - R_1 i_1) - L_\sigma i_1\right\} \qquad (16)$$

In the experimental system, it is set T=0.5.

Fig. 7 shows the block diagram of experimental system with the modification. This system can operate two kinds of control: torque control and speed control. The digital controller uses a DSP (μPD77230:NEC), which can treat 32bit floating point calculation and its instruction cycle is 150nsec. Using this DSP, the control period can be realized within 140μsec. The motor constants are the same as those listed in Table 1.

In order to examine the effectiveness of Eq. (16), a preliminary test was conducted. The result is presented in Fig. 8, which shows the secondary flux calculated by Eq. (16).

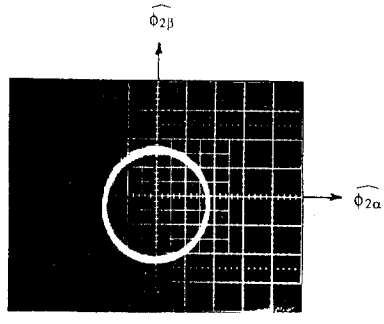

Fig. 8. Trace of estimated secondary flux (at N_r=840rpm)

4.2 Result of torque control

Fig. 9 shows the dynamic response of the proposed torque control system, where the torque command T_q^* was stepwisely changed from positive direction to negative direction. Though the motor speed Nr crosses zero speed, $\widehat{\omega_s}$ follows ω_s^* very well and the response of Nr is very smooth.

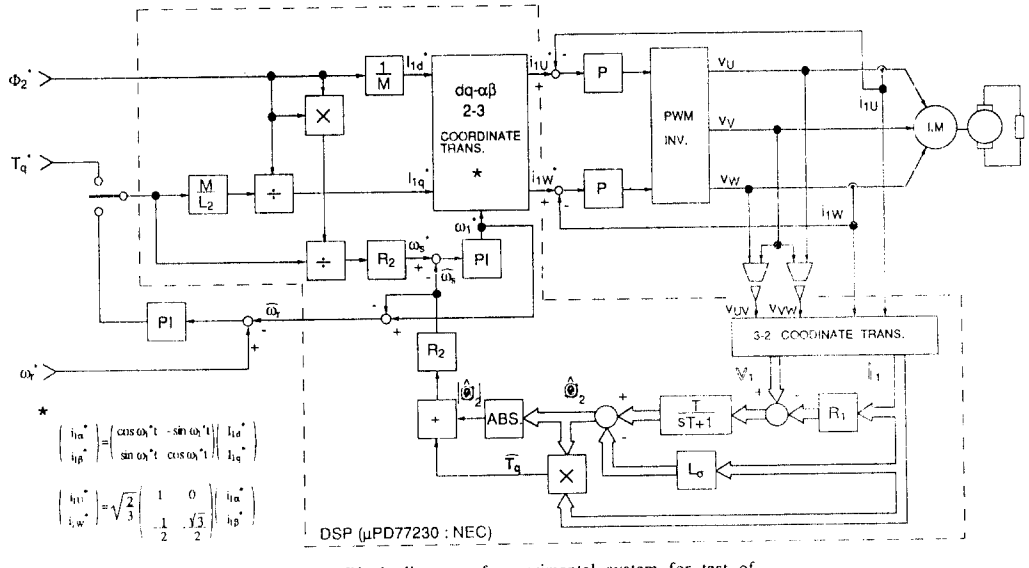

Fig. 7. Block diagram of experimental system for test of torque/speed control

4.3 Result of speed control

Fig. 10 shows the relation N_r^* and N_r, where N_r^* is the command value of the motor speed and N_r is the actual motor speed measured by the speed sensor. Since the relation is linear, it is known that precise speed control is achieved without any speed sensor.

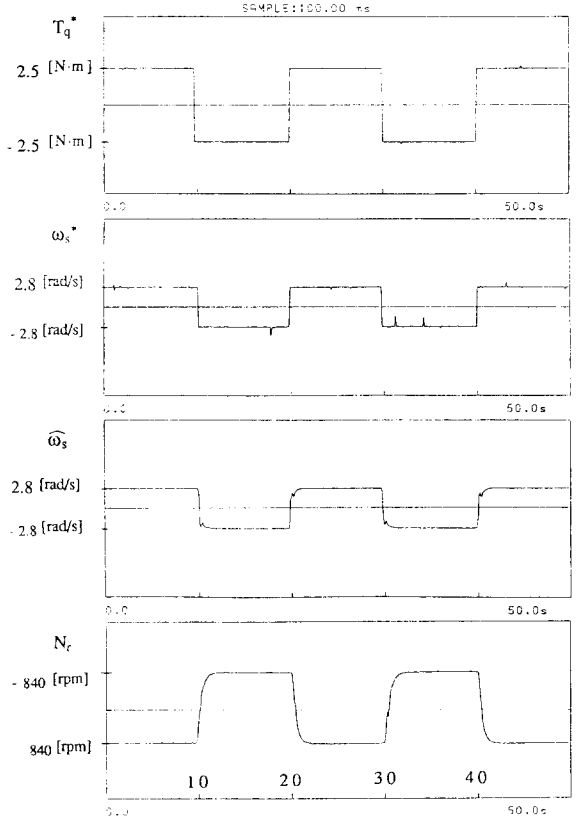

Fig. 9. Experimental result of torque control

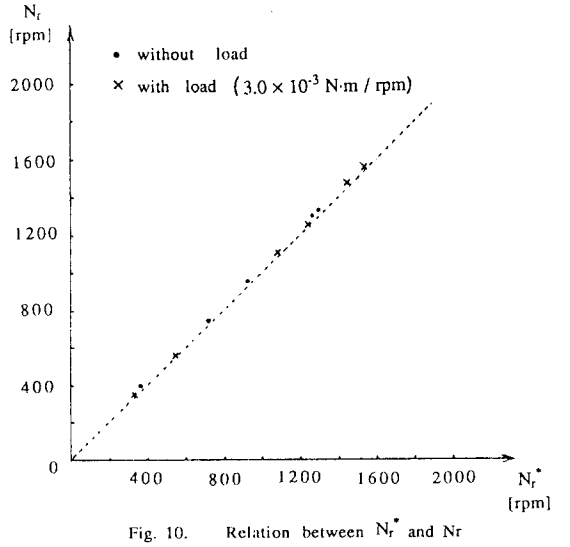

Fig. 10. Relation between N_r^* and Nr

Fig. 11 shows the dynamic response of the proposed speed control system. Though N_r has over shoot, the error of the static value of N_r and N_r^* is within 4%.

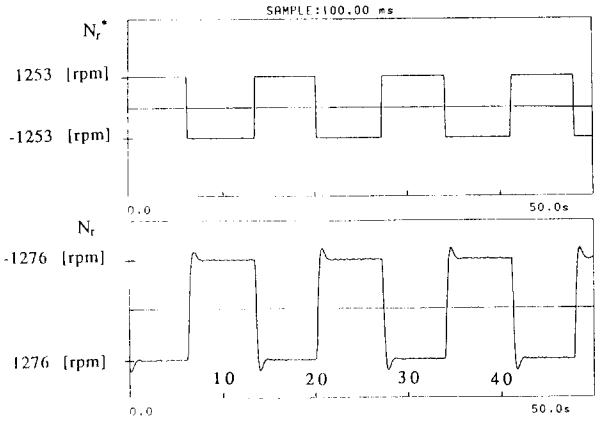

Fig. 11. Experimental result of speed control

5. conclusion

By the simulation and experiment results, we showed that the proposed method is able to realize torque and speed control. The speed error was realized within 4% between 300rpm and 1500rpm.

Reference

[1] A.Abondanti, M.B.Brennen: "Variable Speed Induction Motor Drives Use Electric Slip Calculator Based on Motor Voltages and Currents", IEEE Trans. Vol.IA-11, No.5, pp483-488, 1975

[2] A.Nabae, I.Takahashi, H.Akagi, H.Nakano: "Inverter-fed Induction Motor Drive Systems with an Instantaneous Slip-Frequency Estimation Circuit", IEEE PESC'82, 1982

[3] D.Naunin: "Digital Speed Control of an Induction Motor with and without Speed Sensor", IPEC-Tokyo'83, 1983.3

[4] T.Ohtani, N.Takada, K.Tanaka: "Vector Control of Induction Motor without Shaft Encoder", IEEE IAS'89 Records, pp501-507, 1989.10

[5] F.Harashima, S.Kondo, K.Ohnishi, M.Kajita, M.Susono: "Multi-Microprocessor Based Control System for Quick Response Induction Motor Drive", IEEE IAS'84 Records, pp605-611, 1984.10

[6] F.Harashima, S.Kondo, E.Hachiken, Y.Ohno, K.Ohnishi: "Synchronous Watt Torque Feedback Control of Induction Motor Drives", IEEE IAS '87 Records, pp156-162, 1987.10

[7] H.Hashimoto, Y, Ohno, S.Kondo, F.Harashima: "Torque and Flux Feedback Control of Induction Motor Based on Discrete Model", IEEE IECON'88, pp509-517, 1988.12